lubricants

MDPI

Article

Discussion of Stick-Slip Dynamics of 2DOF Sliding Systems Based on Dynamic Vibration Absorbers Analysis

Satoru Maegawa *, Xiaoxu Liu and Fumihiro Itoigawa

Department of Electrical and Mechanical Engineering, Nagoya Institute of Technology, Gokiso-cho Showa, Nagoya 466-8555, Aichi, Japan; ryu.gyogyoku@nitech.ac.jp (X.L.); itoigawa.fumihiro@nitech.ac.jp (F.I.)
* Correspondence: maegawa.satoru@nitech.ac.jp; Tel./Fax: +81-857-31-5336

Abstract: In this study, we discussed the occurrence condition stick-slip model based on a 2DOF system, in which a 1DOF system model commonly used in stick-slip analysis was attached on an elastic foundation. Specifically, the effects of the mass, stiffness, and damping coefficient of the elastic foundation on the occurrence and non-occurrence of stick-slip were investigated. It was found that when the elastic foundation parameters were determined based on the optimal parameter tuning method of the dynamic vibration absorber (DVA) theory, the range of stick-slip occurrences reduced compared to the sliding system without the elastic foundation.

Keywords: stick–slip; dynamic vibration absorber; sliding friction; vibration suppression

Citation: Maegawa, S.; Liu, X.; Itoigawa, F. Discussion of Stick-Slip Dynamics of 2DOF Sliding Systems Based on Dynamic Vibration Absorbers Analysis. *Lubricants* **2022**, *10*, 113. https://doi.org/10.3390/lubricants10060113

Received: 1 May 2022
Accepted: 30 May 2022
Published: 2 June 2022

1. Introduction

The occurrence of stick-slip inhibits the smooth motion of sliders and causes undesirable vibration and noise in mechanical systems. Therefore, it is important to understand the condition of stick-slip occurrence and develop design guidelines for suppressing it. Stick-slip is often observed in rubber sliding parts such as windshield wipers [1,2] and rubber belts [3,4]. In addition, stick-slip is observed in many industrial products, including automotive parts such as disc brakes and clutches [5,6]. Other examples of stick-slip occurrences that should be prevented are, for example, vibration isolators installed in structures [7–9]. A historical review of stick-slip phenomena and its analysis is provided by Feeny et al. [10].

The occurrence conditions for stick-slip are formulated using several simplified analytical models. For example, Nakano [11] theoretically derived the occurrence criteria for stick-slip using a simplified one-degree-of-freedom vibration system with the Coulomb friction law. By extending the fundamental stick-slip theory, the impact of other parameters on stick-slip occurrence conditions were also studied, including the velocity dependence of the friction coefficient [12], rigidity anisotropy of the support parts [13], and tangential contact compliance [14].

In general, actual vibration systems are often more complex than 1DOF systems, and of course, the phenomena are more complex. However, a slight change in the model from a 1-DOF system to a 2-DOF system makes it impossible to analytically derive the conditions for stick-slip occurrence. It is impossible to derive a stick-slip prediction equation that covers the entire parameter space, and an analytical treatment is possible only in q subspace with some fixed parameters [14]. Currently, when a stick-slip analysis is performed under multi-DOF systems, the parameter range needs to be limited by considering the target system and to derive a simpler design equation within that range.

Dynamic vibration absorbers (DVAs) are effective engineering technologies for controlling vibrating systems [15–18]. Maegawa et al. [18] quantified the stick-slip suppression effect of the DVA using a simplified analytical model based on the stick-slip theory derived by Nakano [11] and the fundamental DVA theory [19]. Maegawa et al. [18] theoretically

demonstrated that appropriately setting the design parameters of the DVA can narrow the stick-slip occurrence area.

In this study, we aimed to discuss the stick-slip dynamics of 2DOF systems using the DVA theory. Figure 1 shows the analytical model used in this study. The model corresponds to the case of a sliding system with the sliding surface fixed to an elastic foundation, as shown in Figure 2. Through numerical simulation and theoretical analysis, in this study, the following two results were obtained. First, the numerical simulation results show that a vibration system attached to an elastic foundation with optimal parameters tuned by the dynamic absorber theory has a reduced region of stick-slip conditions compared to that attached to a rigid base. The stick-slip suppression effect was quantitatively verified by analysis using an equivalent 1DOF vibration system model.

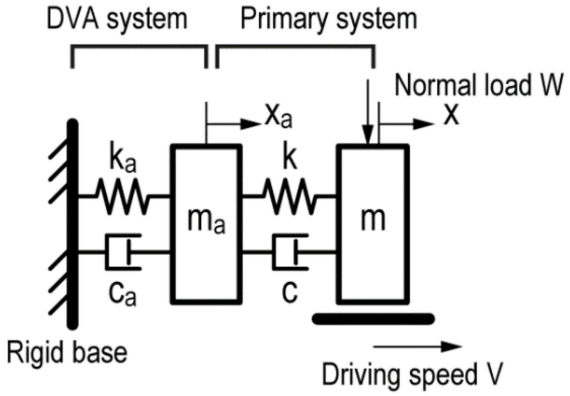

Figure 1. Analytical models in this study.

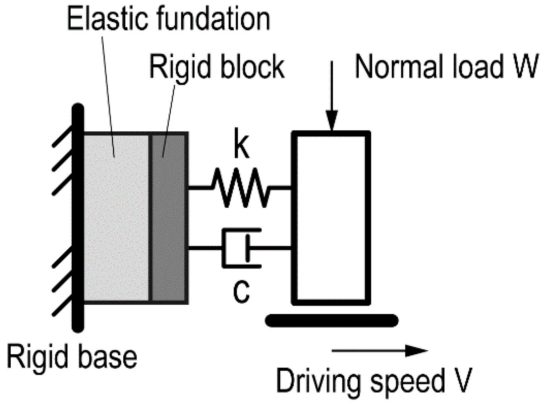

Figure 2. Physical analogue of the analytical model in the present study.

2. Modeling

2.1. Analytical Model

As shown in Figure 1, the analytical model consists of the following two component systems: a primary vibration system and a DVA system (i.e., an elastic foundation system). In the DVA system, an additional mass m_a is connected to the rigid base by a linear spring with a stiffness k_a and a dashpot with a damping coefficient c_a. In the primary vibration system, a primary mass m is then connected in a series to the additional mass m_a by a linear spring with a stiffness k and a dashpot with a damping coefficient c. The mass in the primary system is in contact with a moving plate that moves horizontally with a constant driving speed V under a normal load W. The friction force F acts on the contact interface between the mass and the moving plate.

The effectiveness of the DVA when no friction force acts in the contact interface, as represented in Figure 1, was studied by Harik and Issa [20]. They derived the optimal tuning parameters for the DVA system using a numerical analysis. We build on the research

of Harik and Issa [20] by investigating the effectiveness of the DVA system at suppressing stick-slip in a new configuration, with a friction surface added to the DVA system.

2.2. Governing Equations

The equations of motion for the primary and DVA masses are as follows:

$$\begin{aligned} &m\ddot{x} + c(\dot{x} - \dot{x}_a) + k(x - x_a) = F \\ &m_a\ddot{x}_a - c(\dot{x} - \dot{x}_a) - k(x - x_a) + c_a\dot{x}_a + k_a x_a = 0 \end{aligned} \tag{1}$$

where x and x_a denote the displacement from the natural length of the springs of the primary and additional masses, respectively, and ($^\bullet$) denotes the derivative with respect to time t.

The direction of F is determined by the direction of the relative speed between $\dot{x}$ and V. For the stick state ($\dot{x} = V$), in which static friction F_s acts on the contact surface, it acts along the positive direction of x. In contrast, for the slip-I state ($\dot{x} < V$) and slip-II state ($\dot{x} > V$), kinetic friction F_k acts along the positive and negative directions, respectively. Therefore, F in Equation (1) can be expressed as follows:

$$F = \begin{cases} F_\mathrm{s} & \text{when } \dot{x} = V \quad \text{stick state} \\ F_\mathrm{k} & \text{when } \dot{x} < V \quad \text{slip} - \text{I state} \\ -F_\mathrm{k} & \text{when } \dot{x} > V \quad \text{slip} - \text{II state} \end{cases} \tag{2}$$

During the stick state, the magnitude of F_s is lower than the maximum static friction force F_smax. Thus, the following equation can be written with the static friction coefficient μ_s:

$$-\mu_\mathrm{s}W = -F_\mathrm{smax} \le F_\mathrm{s} \le F_\mathrm{smax} = \mu_\mathrm{s}W \tag{3}$$

When F_s approaches $\mu_\mathrm{s}W$, the friction state changes from the stick state to the slip-I state. During the slip-I and slip-II states, F_k can be expressed using the kinetic friction coefficient μ_k as follows:

$$F_\mathrm{k} = \mu_\mathrm{k}W \tag{4}$$

For simplicity, the Coulomb friction law can be used to express the friction characteristics. Thus, the static and kinetic friction coefficients have different values, with the static coefficient always being larger than the kinetic one. The value of kinetic friction remains constant regardless of changes in the relative speed between $\dot{x}$ and V. The frictional characteristics based on the Coulomb friction law can be summarized as follows:

$$\mu = \begin{cases} \mu_\mathrm{s} = \text{const. when } \dot{x} = V & \text{stick state} \\ \mu_\mathrm{k} = \text{const. when } \dot{x} \neq V & \text{slip-I or slip-II states} \end{cases} \tag{5}$$

Summarizing the above equations, the motion of each mass in the static state can be described by the following governing equations:

$$\dot{x} = V \tag{6}$$

$$-\mu_\mathrm{s}W \le c(V - \dot{x}_a) + k(x - x_a) \le \mu_\mathrm{s}W \tag{7}$$

$$m_a\ddot{x}_a - c(V - \dot{x}_a) - k(x - x_a) + c_a\dot{x}_a + k_a x_a = 0 \tag{8}$$

Additionally, the governing equations for the slip-I state ($\dot{x} < V$) and slip-II state ($\dot{x} > V$) can be written as:

$$\dot{x} < V \tag{9}$$

$$m\ddot{x} + c(\dot{x} - \dot{x}_a) + k(x - x_a) = \mu_\mathrm{k}W \tag{10}$$

$$m_a\ddot{x}_a - c(\dot{x} - \dot{x}_a) - k(x - x_a) + c_a\dot{x}_a + k_a x_a = 0 \tag{11}$$

$$\dot{x} > V \tag{12}$$

$$m\ddot{x} + c(\dot{x} - \dot{x}_a) + k(x - x_a) = -\mu_k W \tag{13}$$

$$m_a\ddot{x}_a - c(\dot{x} - \dot{x}_a) - k(x - x_a) + c_a\dot{x}_a + k_a x_a = 0 \tag{14}$$

where Equations (9)–(11) describe slip state-I, and Equations (12)–(14) describe slip state-II.

2.3. Dimensionless Description of Governing Equations

For a stick-slip analysis using a simplified model, a dimensionless analysis is an effective tool to identify the essential parameters characterizing dynamic behavior and to theoretically derive the occurrence condition [11]. To obtain the governing equations of motion in a dimensionless form, we defined the dimensionless displacements ξ and ξ_a and dimensionless time τ, as follows:

$$\xi = \frac{\omega_n}{V}\left(x - \frac{\mu_k W}{k} - \frac{\mu_k W}{k_a}\right) \tag{15}$$

$$\xi_a = \frac{\omega_n}{V}\left(x_a - \frac{\mu_k W}{k_a}\right) \tag{16}$$

$$\tau = \omega_n t \tag{17}$$

Where ω_n is the natural frequency of the primary vibration system (rad/s), defined as:

$$\omega_n = \sqrt{\frac{k}{m}} \tag{18}$$

Using the dimensionless variables ξ, ξ_a, and τ, the governing equations, Equations (6)–(14), can be rewritten as follows:

$$\xi' = 1 \tag{19}$$

$$-\lambda - 2\gamma\lambda \le 2\zeta(1 - \xi'_a) + \xi - \xi_a \le \lambda \tag{20}$$

$$M\xi''_a - 2\zeta + 2\zeta\xi'_a + 2\zeta_a\xi'_a - \xi + \xi_a + K^2\xi_a = 0 \tag{21}$$

$$\xi' < 1 \tag{22}$$

$$\xi'' + 2\zeta\xi' - 2\zeta\xi'_a + \xi - \xi_a = 0 \tag{23}$$

$$M\xi''_a - 2\zeta\xi' + 2\zeta\xi'_a + 2\zeta_a\xi'_a - \xi + \xi_a + K^2\xi_a = 0 \tag{24}$$

$$\xi' > 1 \tag{25}$$

$$\xi'' + 2\zeta\xi' - 2\zeta\xi'_a + \xi - \xi_a = -2\gamma\lambda \tag{26}$$

$$M\xi''_a - 2\zeta\xi' + 2\zeta\xi'_a + 2\zeta_a\xi'_a - \xi + \xi_a + K^2\xi_a = 0 \tag{27}$$

where $(')$ denotes the derivative with respect to dimensionless time τ, and the dimensionless parameters, M, K, ζ_a, ζ, λ, and γ are defined as follows:

$$M = \frac{m_a}{m}$$

$$K = \sqrt{\frac{k_a}{k}}$$

$$\zeta_a = \frac{c_a}{2\sqrt{mk}}$$

$$\zeta = \frac{c}{2\sqrt{mk}}$$

$$\lambda = \frac{(\mu_s - \mu_k)W}{V\sqrt{mk}}$$

$$\gamma = \frac{\mu_k}{\mu_s - \mu_k}$$

From the dimensionless analysis, it was found that the dynamics in the analytical model shown in Figure 1 can be characterized using only six dimensionless parameters, M, K, ζ_a, ζ, λ, and γ.

Harik and Issa [20] quantified the vibration suppression effect of the DVA in a configuration similar to the one used in this study, but without a sliding surface. In their model, a harmonic external force f_{ext} was applied to the primary mass, as shown in Figure 3. The equation of motion for the analysis model shown in Figure 3 is the same as when the friction force F in Equation (1) is replaced with the periodic excitation force f_{ext} (=$f\sin(\omega t)$), where f and ω are the amplitude and angular frequency, respectively, of the periodic external force.

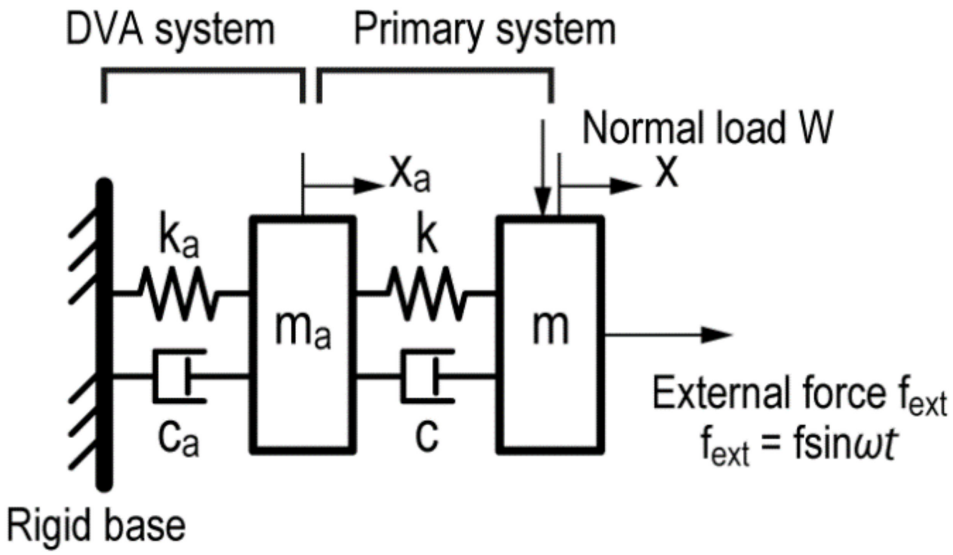

Figure 3. Analytical model in this study without the sliding surface and with a periodic external force f_{ext} applied at the primary mass.

Using numerical techniques, Harik and Issa [20] found an optimally tuned mass ratio M_{opt} (=m_{a_opt}/m), optimally tuned stiffness ratio K_{opt} (=k_{a_opt}/k), and optimally tuned damping ratio ζ_{aopt} (=$c_{a\_opt}/(mk)^{0.5}$) under different damping ratio ζ (=$c/(mk)^{0.5}$) values. As shown in Figure 4, we calculated a best fit curve for the results of Harik and Issa [20] to determine the ζ dependence for each optimally tuned parameter. The resulting formulae are as follows:

$$M_{opt} = 330\zeta^3 - 43.6\zeta^2 + 14.5\zeta + 1.48 \quad (28)$$

$$K_{opt} = 7.72\zeta^3 + 1.13\zeta^2 + 1.38\zeta + 0.934 \quad (29)$$

$$\zeta_{aopt} = 61.1\zeta^3 - 4.40\zeta^2 + 3.91\zeta + 1.09 \quad (30)$$

Figure 5 shows the vibration response curve under different DVA parameter conditions with ζ = 0.1, where H (=kx/f) and Ω (=ω/ω_n) are the dimensionless displacement and the forced frequency ratio, respectively; H_{max} is the maximum dimensionless displacement under each condition. As seen in Figure 5, H_{max} is greatly reduced when the optimally tuned DVA parameters are applied.

Additionally, we calculated a best fit curve for the results from Harik and Issa [20] to determine the ζ dependence of H_{max}, as shown in Figure 6. We obtained the following formula:

$$H_{max} = 2.31\zeta^3 + 0.70\zeta^2 - 3.08\zeta + 2.24 \quad (31)$$

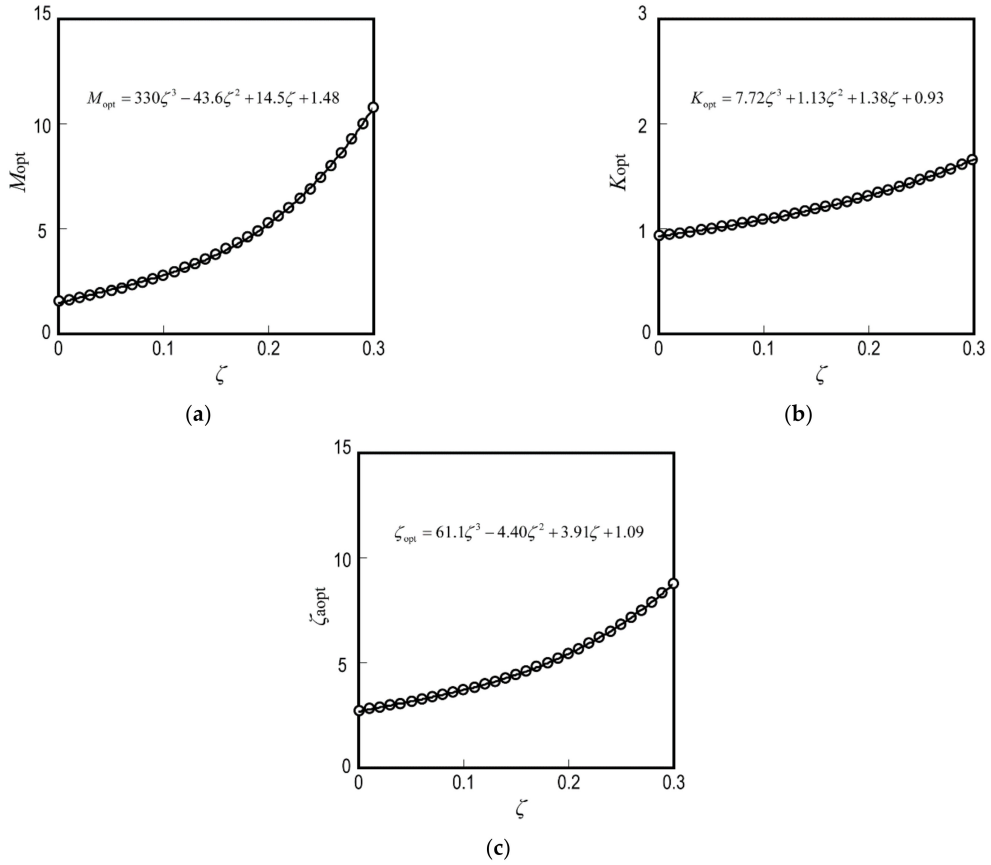

Figure 4. Optimally tuned DVA parameters depending on ζ in the analytical model shown in Figure 3; the open circles show the numerical results derived in [20] and the solid curves show the approximate formula shown in Equations (28)–(30). (**a**) Effect of ζ on M_{opt}, (**b**) Effect of ζ on K_{opt}, (**c**) Effect of ζ on ζ_{a_opt}.

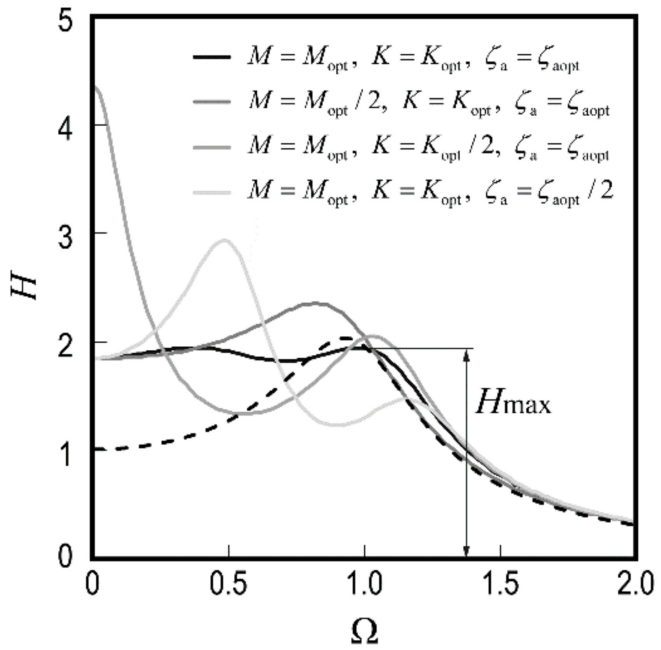

Figure 5. Vibration response curve under the different DVA parameter conditions; dashed line shows vibration response curve with equivalent 1DOF vibration system with ζ_{eq}.

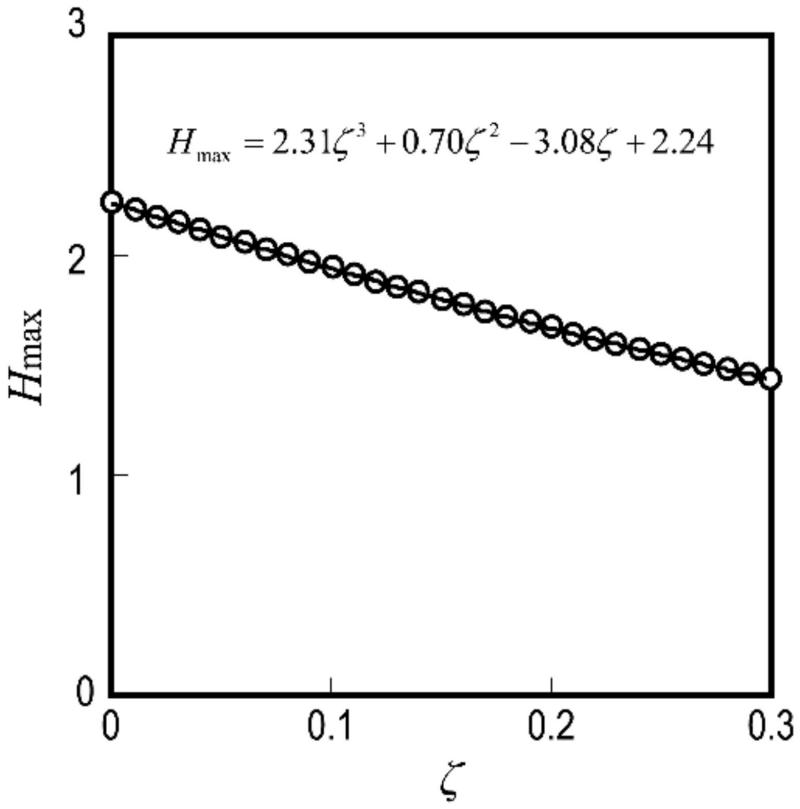

Figure 6. Effect of ζ on $H_{\max}$ under the optimal DVA condition.

This study examines the conditions for stick-slip occurrence when elastic foundations are designed based on the optimal parameters of the dynamic absorber obtained by Harak. Specifically, stick-slip occurrence conditions are calculated when a 1DOF vibration system is attached to an elastic foundation with optimal parameters, and stick-slip occurrence conditions are calculated when a 1DOF vibration system is directly attached to a rigid base, and the two are compared.

3. Numerical Results

Numerical simulations, also referred to as time variations in ξ, were performed to quantify the stick-slip suppression effect of optimally tuned elastic foundations. Using the dimensionless equations of motion, provided by Equations (19)–(27), the time variations in the dimensionless displacement of the primary mass ξ were solved numerically with the Runge–Kutta method.

Figure 7 shows the results of the numerical simulation. The parameters were set as follows: (a) $M = M_{\text{opt}}$, $K = K_{\text{opt}}$, $\zeta_a = \zeta_{a\text{opt}}$, $\zeta = 0.1$, and $\gamma = 2$, and (b) $M = M_{\text{opt}}$, $K = 2K_{\text{opt}}$, $\zeta_a = \zeta_{a\text{opt}}$, $\zeta = 0.1$, and $\gamma = 2$. Thus, the results in Figure 7a,b correspond to the use of the optimally tuned DVA and the non-optimally tuned DVA systems, respectively. Previous research shows that stick-slip occurs under a large λ condition [11]. Considering that an increase in λ corresponds to an increase in the normal load W, a decrease in velocity V, and a decrease in support stiffness k, the observed stick-slip characteristics exhibit typical stick-slip behavior. Figure 7 clearly shows that setting the value for the DVA parameter strongly affects the occurrence and non-occurrence of stick-slip.

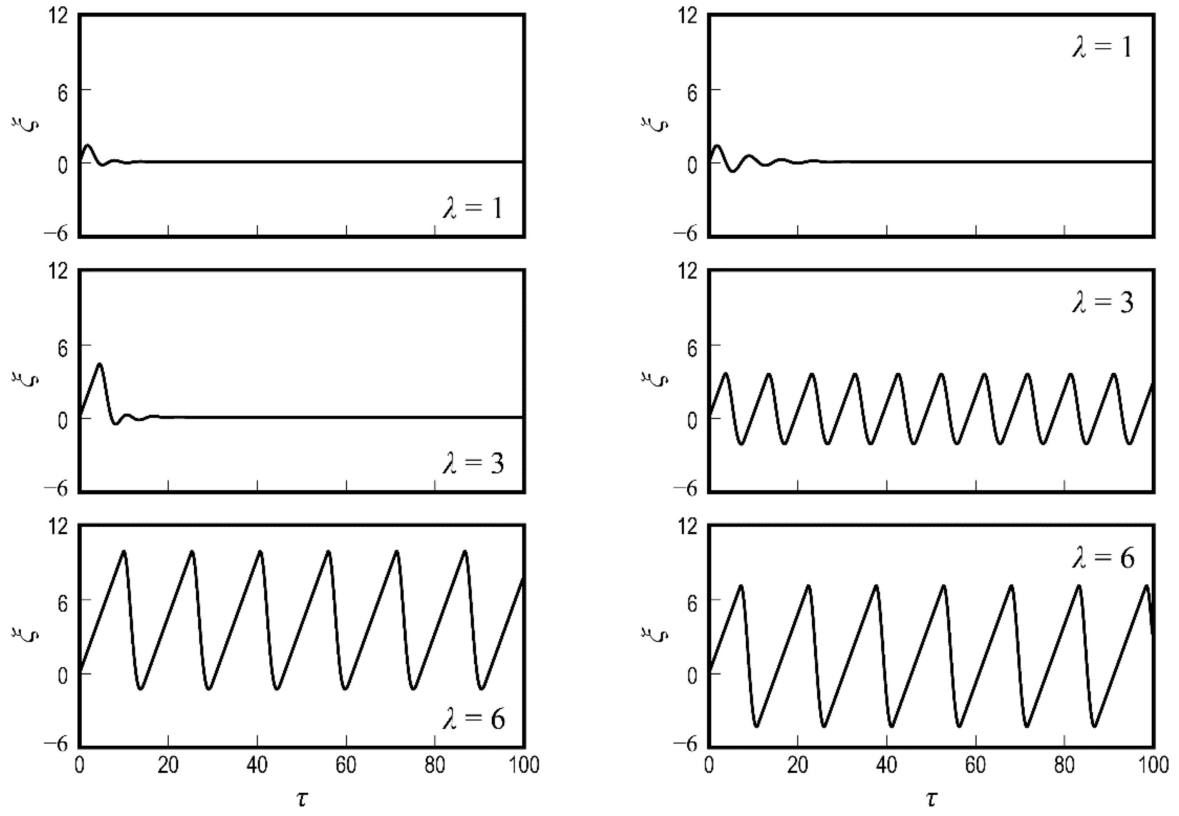

(**a**) With optimally tuned DVA (**b**) With non-optimally tuned DVA

Figure 7. Time variations of dimensionless displacement ξ under different λ with (**a**) optimally tuned DVA ($M = M_{opt}$, $K = K_{opt}$, $\zeta_a = \zeta_{aopt}$, $\zeta = 0.1$ *and* $\gamma = 2$) and (**b**) non-optimally tuned DVA ($M = M_{opt}$, $K = 2K_{opt}$, $\zeta_a = \zeta_{aopt}$, $\zeta = 0.1$ and $\gamma = 2$).

As derived from the dimensionless analysis in Section 2.3, the dynamic behavior of the analysis system shown in Figure 1 can be determined using only the six parameters, i.e., M, K, ζ_a, ζ, λ, and γ. Because the DVA parameters are optimally set based on Equations (28)–(30), that is, M_{aopt}, K_{aopt}, and ζ_{aopt} are the dependent variables of ζ, the dynamic behavior of the present system is characterized only by the three parameters λ, ζ, and γ. Because γ does not affect the occurrence and non-occurrence of stick-slip [11], it is possible to completely determine when stick-slip occurs by investigating the occurrence and non-occurrence of stick-slip when λ and ζ are changed.

Figure 8 shows the effect of the use of the DVA on the occurrence and non-occurrence conditions of stick-slip based on the results of the numerical simulation with $\gamma = 2$. The results shown in Figure 8a are based on the results of the numerical simulation when the 1DOF vibration system is directly attached to the rigid base. This figure corresponds to the stick-slip occurrence/non-occurrence map for the equivalent one-degree-of-freedom vibration system shown later in Figure 9, when $c_{eq} = 0$. Thus, this configuration corresponds to the stick-slip occurrence condition when no DVA is used. The solid line drawn in Figure 8a is the discriminant equation of the boundary conditions for the occurrence and non-occurrence of stick-slip when not using the DVA system, based on Equation (37).

In contrast, in Figure 8b, the stick-slip occurrence condition was determined by the numerical simulation of the optimally tuned DVA vibration system shown in Figure 1, where the solid line in Figure 8b is based on Equation (37). That is, it is the map of stick-slip occurrence and non-occurrence conditions when the parameters of the elastic foundation are set to optimal values based on dynamic absorber theory. Comparing Figure 8a,b, the use of the optimized DVA works to narrow the stick-slip region under all conditions.

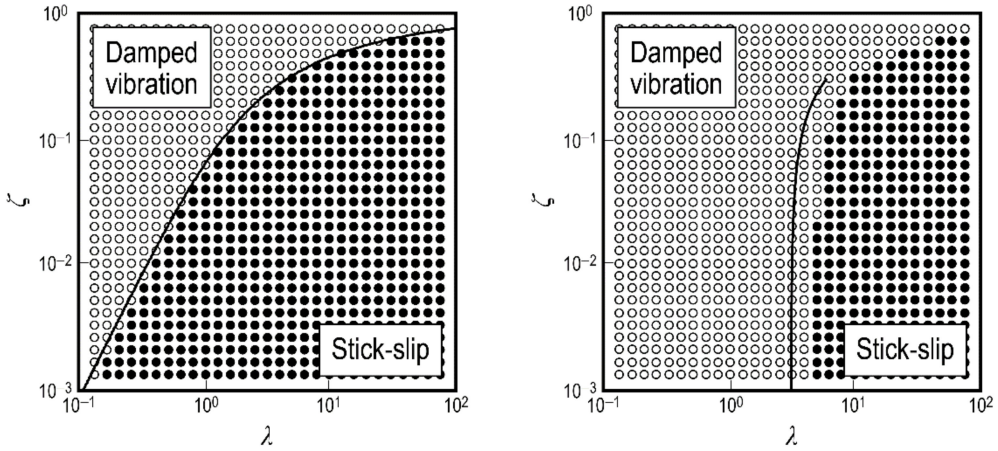

(**a**) without DVA (**b**) with optimally tuned DVA

Figure 8. The occurrence and non-occurrence map of stick-slip obtained by numerical simulation under $\gamma = 2$; the solid circles show the occurrence conditions for stick-slip; the open circles show the non-occurrence conditions of stick-slip (i.e., damped vibration conditions); and the solid curves show the boundary between the occurrence and non-occurrence of stick-slip derived by (**a**) Equation (39), without DVA and (**b**) Equation (37), with optimally tuned DVA.

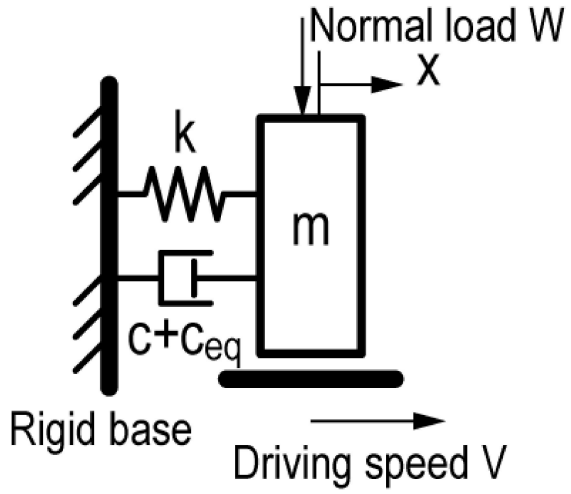

Figure 9. Equivalent one-degree-of-freedom vibration system without the DVA system.

4. Discussion

Figure 8 demonstrates that the use of an optimized elastic foundation suppresses stick-slip occurrence. In this section, the stick-slip suppression effect is quantified.

As described above, the Harik and Issa model [20] harmonic external force f_{ext} ($=f\sin(\omega t)$) was applied to the primary mass, as shown in Figure 3. If the frequency of the cyclic external force is in the region close to the natural frequency of the system (i.e., $\omega = \omega_n$) under the condition that the dynamic absorber parameters are optimized, the behavior of the system can be approximated by an equivalent 1DOF vibration system. Figure 9 shows the equivalent 1DOF system that can replace the 2DOF DVA system shown in Figure 1. In Figure 9, the magnitude of c_{eq} represents the stick-slip suppression effect of the DVA.

The relationship between the maximum dimensionless deflection $H_{\max}$ and the damping ratio of the equivalent model $\zeta_{\text{eq}} = (c + c_{\text{eq}})/(2(mk)^{0.5})$ is given by the following equation:

$$H_{\max} = \frac{1}{2\zeta_{\text{eq}}} \tag{32}$$

From Equations (31) and (32), the equivalent damping ratio can be written as a function of the damping ratio, as follows:

$$\zeta_{\mathrm{eq}} = \frac{1}{4.62\zeta^3 + 1.40\zeta^2 - 6.16\zeta + 4.48} \tag{33}$$

Figure 10 shows the dependence of ζ on ζ_{eq}. Here, ζ_{eq} is the equivalent damping ratio including the damping effect of the optimally applied DVA, and ζ is the damping ratio of the primary vibration system. Therefore, Equation (33) holds only when the DVA is optimally adjusted.

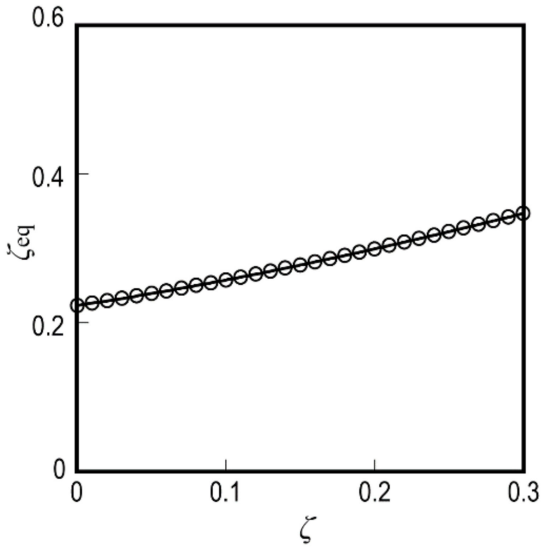

Figure 10. Effect of ζ on ζ_{eq} under optimally tuned DVA condition.

The black solid line in Figure 5 shows the vibration response curve when tuned with the optimal parameters. On the other hand, the dashed line in Figure 5 shows the vibration response curve of the equivalent 1DOF vibration system with ζ_{eq}. From Figure 5, it is found that the behavior of the main vibration system in the 2DOF system and the equivalent 1-DOF system are in good agreement in the range close to $\omega = \omega_n$.

The analysis conducted by Nakano et al. shows that the vibration frequency of stick-slip approaches the natural frequency as λ decreases [14]. When λ is smaller than 1, the vibration frequency of the stick-slip can be approximated by the natural frequency of the system. That is, in this case, the behavior of the system vibrating due to stick-slip coincides with the behavior of the system when it is vibrated by a periodic external force. The only difference is whether the source of the vibration is an external force or the difference between static and dynamic frictional forces.

If λ is smaller than 1, the vibration frequency of stick-slip can be approximated by the natural frequency of the system. In other words, in this case, the behavior of the system vibrating due to stick-slip is consistent with the behavior of the system when it is vibrating due to periodic external forces. Although the switching between static and dynamic frictional forces excites the system, the behavior of the system is the same as when subjected to a sinusoidal external excitation force. It should be noted that the1DOF vibration system used in this study is only equivalent when λ has relatively small values as described above. When λ is small, the vibration waveform of the stick-slip becomes a harmonic vibration, increasing the applicability of the theory for quantifying the optimum parameter of the DVA. In the 1DOF system, the λ dependence of the stick-slip frequency f_{ss} and amplitude A_{ss} is formulated as follows

$$\frac{f_{ss}}{f_n} = \left\{1 + \frac{1}{\pi}(\lambda - \tan^{-1}\lambda)\right\}^{-1} = \begin{cases} 1 & \text{for small } \lambda \\ \pi\lambda^{-1} & \text{for large } \lambda \end{cases} \tag{34}$$

$$\frac{A_{ss}}{A_n} = \sqrt{1+\lambda^2} = \begin{cases} 1 & \text{for small } \lambda \\ \lambda & \text{for large } \lambda \end{cases} \tag{35}$$

where $f_n = \omega_n/2\pi$ and $A_n = V/\omega_n$.

Nakano's [11] boundary equation for the occurrence and non-occurrence conditions of stick-slip for the 1DOF system with Coulomb friction is applied to the equivalent model shown in Figure 9. The boundary equation of the equivalent model can thus be written using the two dimensionless parameters, λ and ζ_{eq}, as follows:

$$\ln\left(1 - 2\zeta_{eq}\lambda + \lambda^2\right) = \frac{\zeta_{eq}}{\sqrt{1-{\zeta_{eq}}^2}}\left(3\pi + 2\tan^{-1}\frac{1-\zeta_{eq}\lambda}{\lambda\sqrt{1-{\zeta_{eq}}^2}}\right) \tag{36}$$

Equation (36) can be expressed in the more simplified form [11]:

$$\frac{(1-\zeta_{eq})^5}{\zeta_{eq}}\lambda^2 = 4\pi \tag{37}$$

From Equation (37), the criterion for preventing the occurrence of stick-slip in this configuration can be written as:

$$\frac{(1-\zeta_{eq})^5}{\zeta_{eq}}\lambda^2 < 4\pi \tag{38}$$

When the DVA is not installed, $c_{eq} = 0$ in the equivalent model shown in Figure 9. Thus, the results in Figure 8a corresponds to the results of stick-slip occurrence conditions when $c_{eq} = 0$ in Figure 9. Therefore, by replacing ζ_{eq} with ζ in Equation (37), it is possible to obtain the boundary equation for the occurrence and non-occurrence of stick-slip when the DVA is not attached, as shown below:

$$\frac{(1-\zeta)^5}{\zeta}\lambda^2 = 4\pi \tag{39}$$

Using Equations (33) and (37), we determined the occurrence criteria for stick-slip based on the two dimensionless parameters λ and ζ.

The procedure used to determine the stick-slip occurrence condition for a sliding surface for which ζ is known is recounted here. First, the optimum values of the dimensionless parameters (M_{opt}, K_{opt}, ζ_{aopt}) were determined using Equations (28)–(30). At the same time, the optimum value of the DVA parameters (m_{a_opt}, k_{a_opt}, c_{a_opt}) were determined using Equations (28)–(30). Using the results, we were able to design a DVA for the specific situation. Based on Equation (33), we quantified the equivalent damping ratio ζ_{eq} when the optimum vibration absorber was installed. Finally, using Equation (38), we were able to quantify the values of λ at which stick-slip occurs. Because λ includes the velocity V and load W, it was possible to quantify the velocity range or normal load range in which stick-slip was expected to occur.

Figure 8b clearly shows that the stick-slip occurrence area is in good agreement with the prediction by the discriminant equation in Equation (37). In other words, the increase in the damping effect improved by the optimal tuning of the elastic foundation (DVA) is considered to have worked to suppress stick-slip. As mentioned above, Equation (37) can predict the occurrence and non-occurrence of stick-slip more accurately when λ is relatively small. On the other hand, when λ is relatively large, the modeling of the equivalent 1DOF vibration system is not appropriate, which may be the reason for the discrepancy between the discriminant equation and the numerical simulation results. The significance of the discriminant equation derived in this study is that it provides a theoretical basis for the fact that the stick-slip suppression effect of a vibration system mounted on an optimally tuned elastic foundation is due to the vibration suppression effect of the DVA, at

least under conditions where λ is small. The numerical simulation results show that the stick-slip occurrence region is only inside the region predicted by Equation (37), indicating that this equation can be used as a discriminant equation to predict stick-slip occurrence and non-occurrence.

The discriminant of Equation (37) is not always valid when the set values of the DVA deviate from the values found using Equations (28)–(30). This is because the equation applies an equivalent one-degree-of-freedom vibration system assuming an optimally tuned dynamic absorber is installed, which would not be appropriate if the parameters are not optimal. Figure 11 shows the stick-slip occurrence and non-occurrence map when a non-optimally tuned DVA system is used. The parameters were set as follows: in Figure 11a, the parameters are set to $M = M_{\mathrm{opt}}$, $K = K_{\mathrm{opt}}/2$, $\zeta_a = \zeta_{a\mathrm{opt}}$, and $\gamma = 2$; and in Figure 11b the parameters are set to $M = M_{\mathrm{opt}}$, $K = 2K_{\mathrm{opt}}$, $\zeta_a = \zeta_{a\mathrm{opt}}$, and $\gamma = 2$. When the parameters of the DVA diverge from those defined by Equations (28)–(30), the stick-slip occurrence region may be wider or narrower than the region predicted by Equation (37). Importantly, the discriminant of Equation (37) does not necessarily show the maximum stick-slip suppression ability of the DVA. The importance of Equation (37) is that if the parameters of the DVA are set to the values defined by Equations (28)–(30), then Equation (37) represents the region where stick-slip reliably does not occur. Thus, the theoretical prediction tool derived in this study can be utilized effectively when making a quantitative design based on theory.

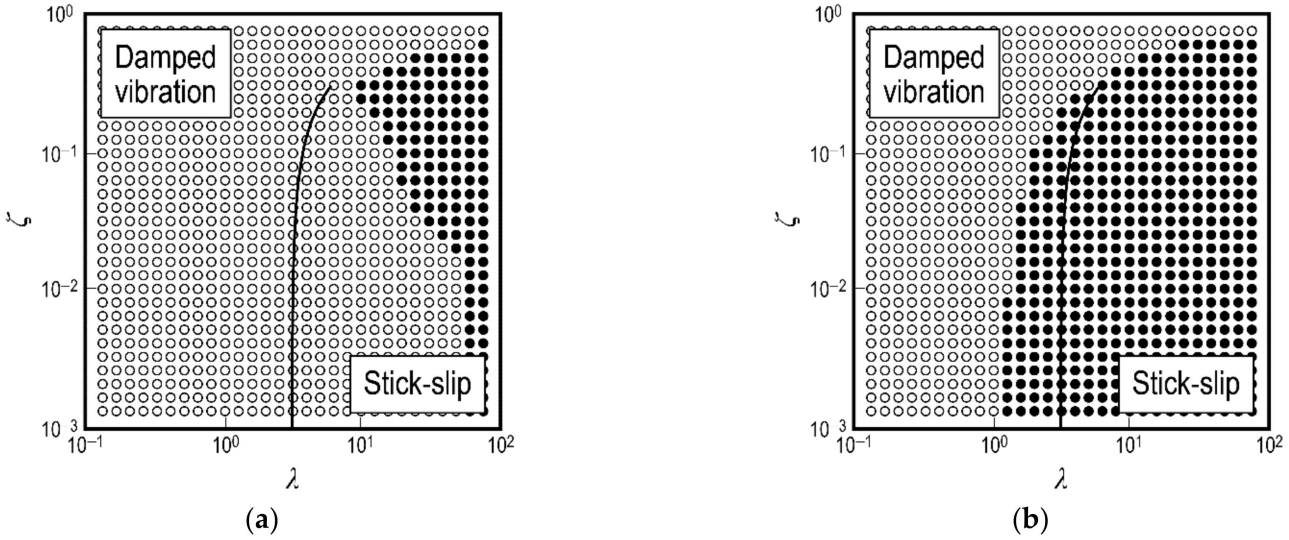

Figure 11. The occurrence and non-occurrence map of stick-slip obtained by numerical simulation under $\gamma = 2$ for investigating the stick-slip suppression effect of non-optimally tuned DVA systems. (**a**) $M = M_{\mathrm{opt}}$, $K = K_{\mathrm{opt}}/2$, $\zeta_a = \zeta_{a\mathrm{opt}}$; (**b**) $M = M_{\mathrm{opt}}$, $K = K_{\mathrm{opt}} \times 2$, $\zeta_a = \zeta_{a\mathrm{opt}}$.

Focusing on the results in Figure 11a, it can be seen that the area of stick-slip occurrence is overwhelmingly narrower than in other conditions, which is a characteristic result. Figure 12 shows the time variations of dimensionless displacements ξ and ξ_a and dimensionless velocities ξ' and ξ'_a under $\lambda = 1$, $\zeta = 0.01$. Under these conditions, stick-slip does not occur in either case and the initial fluctuations decrease and decay with time. A closer look reveals that for $K = K_{\mathrm{opt}}/2$, i.e., Figure 12a, the oscillations of the main vibration system (black line) and the secondary vibration (DVA) system (gray line) are nearly in opposite phases. On the other hand, in case $K = k_{\mathrm{opt}} \times 2$, i.e., Figure 12b, each mass point is oscillating in perfectly in-phase. Figure 13 shows the time variations of dimensionless displacements ξ and ξ_a and dimensionless velocities ξ' and ξ'_a under $\lambda = 10$, $\zeta = 0.01$. In Figure 13a, stick-slip does not occur, but in Figure 13b, stick-slip is observed. This corresponds to the fact that in Figure 11, the stick-slip region is wide for $K = k_{\mathrm{opt}} \times 2$ and extremely narrow for $K = K_{\mathrm{opt}}/2$. From the above, it can be seen that the vibration modes have a significant effect on the stick-slip suppression observed in Figure 11a. In the case

of $K = K_{opt}/2$, the two masses oscillate in opposite phases as a second-order mode, and their motions cancel each other out to produce the stick-slip suppression effect. In this case, stick-slip can be suppressed even at a higher λ than the condition predicted by the stick-slip occurrence discriminant formula shown in Equation (37). In other words, by setting the phases of the two masses well, it is possible to obtain a large vibration suppression effect beyond the vibration suppression effect of a general dynamic absorber. Although this effect is not discussed in depth in this study, it is considered to be an important finding for stick-slip suppression in 2DOF vibration systems.

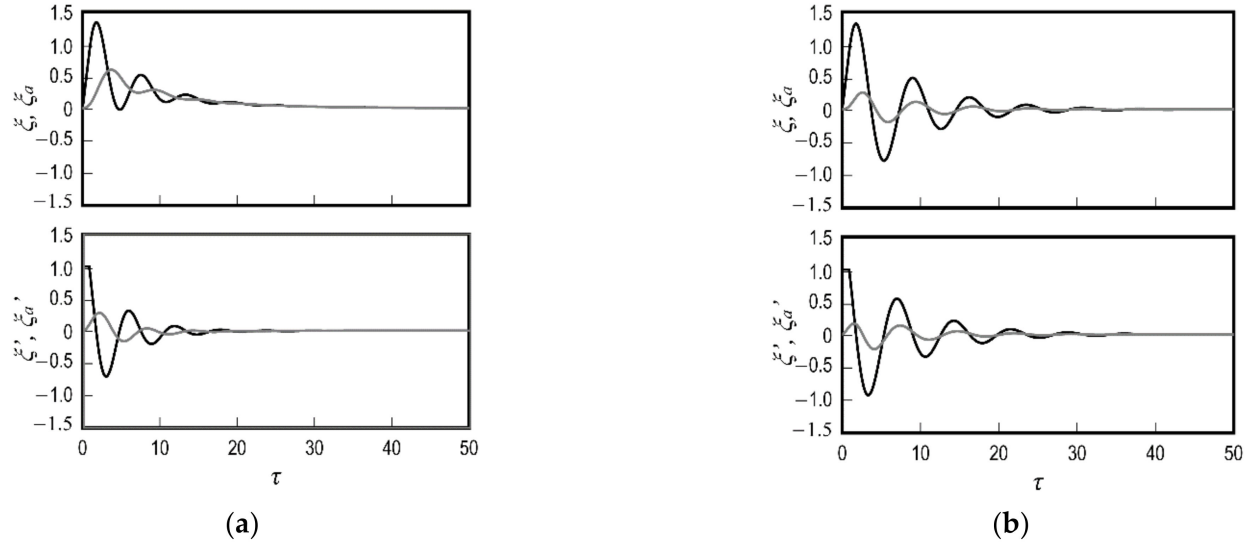

Figure 12. Time variations of dimensionless displacements ξ and ξ_a and dimensionless velocities ξ' and ξ'_a under $\lambda = 1$, $\zeta = 0.01$. (**a**) $M = M_{opt}$, $K = K_{opt}/2$, $\zeta_a = \zeta_{aopt;}$ (**b**) $M = M_{opt}$, $K = K_{opt} \times 2$, $\zeta_a = \zeta_{aopt}$.

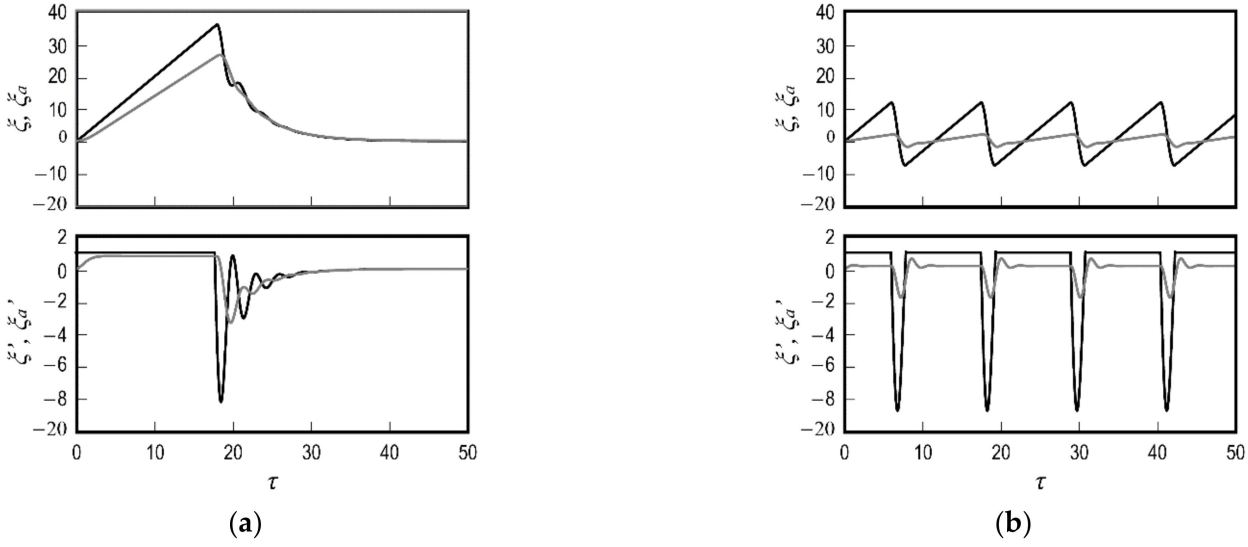

Figure 13. Time variations of dimensionless displacements ξ and ξ_a and dimensionless velocities ξ' and ξ'_a under $\lambda = 10$, $\zeta = 0.01$. (**a**) $M = M_{opt}$, $K = K_{opt}/2$, $\zeta_a = \zeta_{aopt;}$ (**b**) $M = M_{opt}$, $K = K_{opt} \times 2$, $\zeta_a = \zeta_{aopt}$.

Figures 14 and 15 show trajectories in a phase plane with ξ and ξ' an under $\lambda = 1$, $\zeta = 0.01$ and under $\lambda = 10$, $\zeta = 0.01$, respectively. Note that the calculation conditions for Figures 14 and 15 are the same as those for Figures 12 and 13. From the phase plane, the oscillation behavior of the main vibration system can be well understood visually. As shown in Figure 14, under relatively small λ conditions, the oscillations decay gradually, i.e., the orbit spirals toward the origin. On the other hand, for large λ, the behavior changes drastically. In the case of Figure 15a, where stick-slip does not occur, the vibration does not decay in a spiral manner as seen in Figure 14, but instead follows a peculiar trajectory. It is clear that the behavior under the same conditions cannot be approximated by a 1DOF vibration system, and results in the second-order mode of vibration behavior described above. In Figure 15b, where stick-slip occurs, a limit cycle is formed.

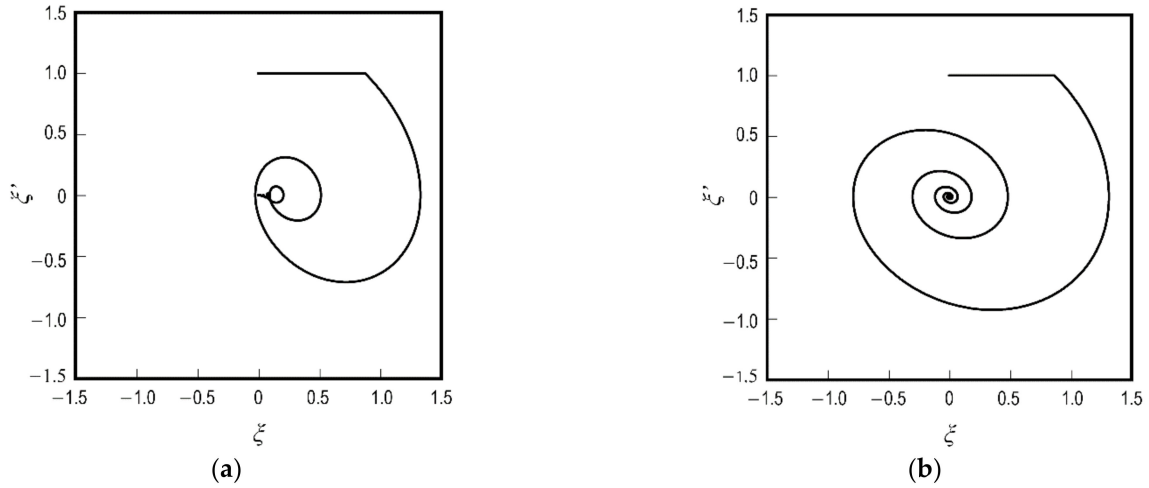

Figure 14. Trajectories in a phase plane with ξ and ξ' an under $\lambda = 1$, $\zeta = 0.01$. (**a**) $M = M_{\mathrm{opt}}$, $K = K_{\mathrm{opt}}/2$, $\zeta_a = \zeta_{a\mathrm{opt}}$; (**b**) $M = M_{\mathrm{opt}}$, $K = K_{\mathrm{opt}} \times 2$, $\zeta_a = \zeta_{a\mathrm{opt}}$.

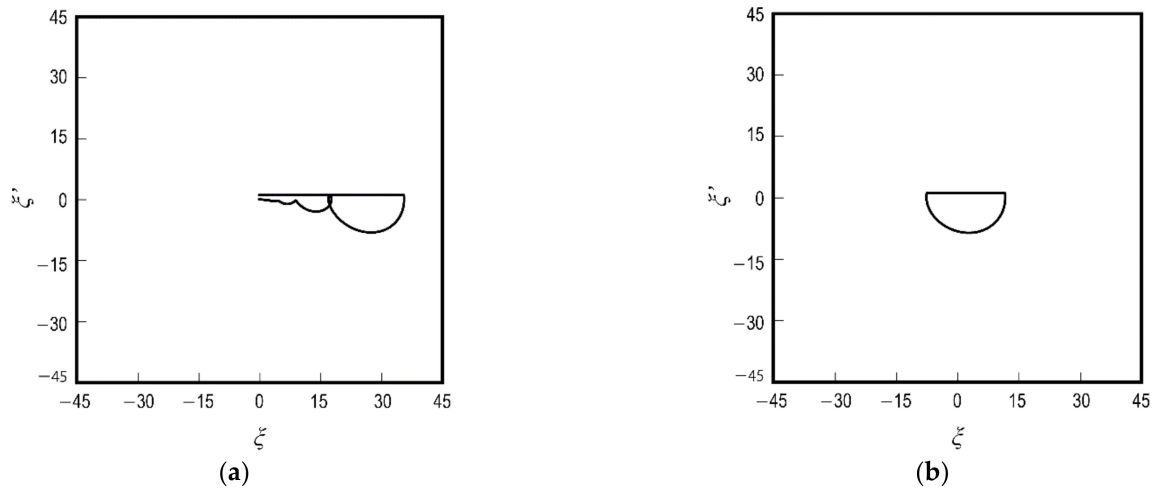

Figure 15. Trajectories in a phase plane with ξ and ξ' an under $\lambda = 10$, $\zeta = 0.01$. (**a**) $M = M_{\mathrm{opt}}$, $K = K_{\mathrm{opt}}/2$, $\zeta_a = \zeta_{a\mathrm{opt}}$; (**b**) $M = M_{\mathrm{opt}}$, $K = K_{\mathrm{opt}} \times 2$, $\zeta_a = \zeta_{a\mathrm{opt}}$.

Finally, Figure 16 shows a design flowchart for stick-slip suppression by attachment to an elastic foundation. The following seven parameters are determined by modeling into a 1DOF sliding system; further, the value of λ and ζ are also obtained. By substituting the estimated ζ into Equation (33) we can obtain ζ_{eq}. Next, λ and ζ_{eq} are substituted into Equation (38). If the same equation holds, stick-slip suppression using an elastic foundation is possible. By substituting ζ into Equations (28)–(30), we can then obtain M_{opt}, K_{opt}, and

ζ_{aopt}. From these, the optimal parameters of the elastic foundation, m_{a_opt}, k_{a_opt}, and c_{a_opt}, are calculated. Finally, we redesign the targeted sliding system based on the obtained design parameters of the sliding system with elastic foundation (DVA).

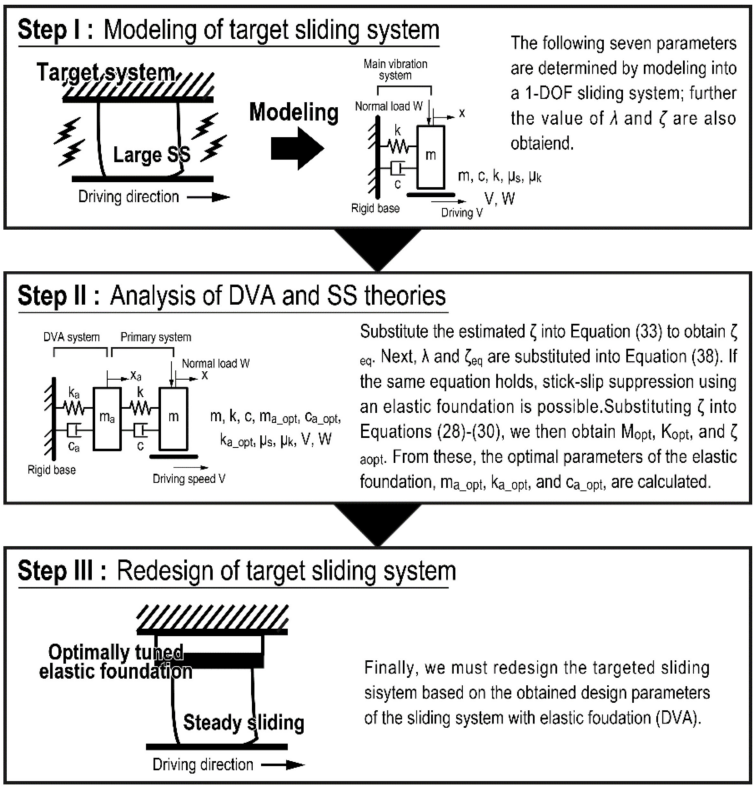

Figure 16. Schematics of the design strategy for suppressing stick-slip using optimally tuned elastic foundation.

5. Conclusions

In this study, the dynamics of stick-slip in a 2-DOF sliding system mounted on an elastic foundation with a typical 1-DOF sliding system with Coulomb friction was discussed. Specifically, it was found that the vibration system mounted on an elastic foundation with optimal parameter tuning based on dynamic absorber theory is more effective in suppressing stick-slip than a vibration system directly mounted on a rigid foundation. The stick-slip suppression effect can be quantitatively evaluated using the stick-slip occurrence/non-occurrence discriminant equation derived in this study. In addition to the above results, this study also discussed the design procedure of the vibration system to suppress stick-slip occurrence using an elastic foundation. Although in this study the mechanism is not perfectly understood, it was found that the conditions for stick-slip occurrence in a 2-DOF vibration system differs greatly depending on the vibration mode. It is considered to be an important finding for stick-slip suppression in 2DOF vibration systems.

Author Contributions: Conceptualization, S.M.; Investigation, S.M.; Supervision, X.L. and F.I.; Writing—original draft, S.M. All authors have read and agreed to the published version of the manuscript.

Funding: This research received no external funding.

Institutional Review Board Statement: Not applicable.

Informed Consent Statement: Not applicable.

Data Availability Statement: The data of numerical simulation of this study are available from the corresponding author upon request.

Acknowledgments: Not applicable.

Conflicts of Interest: The authors declare no conflict of interest.

Abbreviations

List of Symbols (units)

c	damping coefficient of the primary vibration system (N s/m)
c_a	damping coefficient of the DVA system (N s/m)
$c_{\mathrm{a\_opt}}$	optimally tuned damping coefficient of the DVA system (N s/m)
c_{eq}	equivalent damping coefficient
f	amplitude of the periodic external force (N)
f_{ext}	periodic external force (N)
F	friction force (N)
F_{k}	kinetic friction force (N)
F_{s}	static friction force (N)
F_{smax}	maximum static friction force (N)
H	dimensionless displacement under without DVA system
H_{max}	maximum value of H
k	stiffness of the primary vibration system (N/m)
k_a	stiffness of the DVA system (N/m)
$k_{\mathrm{a\_opt}}$	optimally tuned stiffness of the DVA system (N/m)
K	stiffness ratio
K_{opt}	optimally tuned stiffness ratio
m	mass of the primary vibration system (kg)
m_a	additional mass of the DVA system (kg)
$m_{\mathrm{a\_opt}}$	optimally tuned additional mass of the DVA system (kg)
M	mass ratio
M_{opt}	optimally tuned mass ratio
t	time (s)
V	driving speed (m/s)
W	normal load (N)
x	displacement of the primary mass (m)
$\dot{x}$	velocity of the primary mass (m/s)
$\ddot{x}$	acceleration of the primary mass (m/s^2)
x_a	displacement of the additional mass (m)
$\dot{x}_a$	velocity of the additional mass (m/s)
$\ddot{x}_a$	acceleration of the additional mass (m/s^2)
γ	dimensionless parameter
λ	dimensionless parameter
μ_{k}	kinetic friction coefficient
μ_{s}	static friction coefficient
τ	dimensionless time
ω	angular frequency of the periodic external force
ω_n	natural frequency of the primary vibration system (rad/s)
Ω	forced frequency ratio
ξ	dimensionless displacement of the primary mass
ξ'	dimensionless velocity of the primary mass
ξ''	dimensionless acceleration of the primary mass
ξ_a	dimensionless displacement of the additional mass
ξ'_a	dimensionless velocity of the additional mass
ξ''_a	dimensionless acceleration of the additional mass
ζ	damping ratio
ζ_a	damping ratio of the DVA system
ζ_{aopt}	optimally tuned damping ratio of the DVA system
ζ_{eq}	equivalent damping coefficient

References

1. Koenen, A.; Sanon, A. Tribological and vibroacoustic behavior of a contact between rubber and glass (application to wiper blade). *Tribol. Int.* **2007**, *40*, 1484–1491. [CrossRef]
2. Le Rouzic, J.; Le Bot, A.; Perret-Liaudet, J.; Guibert, M.; Rusanov, A.; Douminge, L.; Bretagnol, F.; Mazuyer, D. Friction-induced vibration by Stribeck's law: Application to wiper blade squeal noise. *Tribol. Lett.* **2013**, *49*, 563–572. [CrossRef]
3. Khattab, M.; Wasfy, T. Prediction of Dynamic Stick-Slip Events in Belt-Drives Using a High-Fidelity Finite Element Model. *J. Comput. Nolinear Dynam.* **2022**, *17*, 064501. [CrossRef]
4. Wu, Y.; Leamy, M.J.; Varenberg, M. Minimizing self-oscillation in belt drives: Surface texturing. *Tribol. Int.* **2020**, *145*, 106157. [CrossRef]
5. Lee, S.M.; Shin, M.W.; Lee, W.K.; Jang, H. The correlation between contact stiffness and stick–slip of brake friction materials. *Wear* **2013**, *302*, 1414–1420. [CrossRef]
6. Lazzari, A.; Tonazzi, D.; Conidi, G.; Malmassari, C.; Cerutti, A.; Massi, F. Experimental evaluation of brake pad material propensity to stick-slip and groan noise emission. *Lubricants* **2018**, *6*, 107. [CrossRef]
7. Dolce, M.; Cardone, D.; Croatto, F. Frictional behavior of steel-PTFE interfaces for seismic isolation. *Bull. Earthq. Eng.* **2005**, *3*, 75–99. [CrossRef]
8. Gandelli, E.; De Domenico, D.; Dubini, P.; Besio, M.; Bruschi, E.; Quaglini, V. Influence of the breakaway friction on the seismic response of buildings isolated with curved surface sliders: Parametric study and design recommendations. *Structures* **2020**, *27*, 788–812. [CrossRef]
9. Quaglini, V.; Dubini, P.; Furinghetti, M.; Pavese, A. Assessment of Scale Effects in the Experimental Evaluation of the Coefficient of Friction of Sliding Isolators. *J. Earthq. Eng.* **2019**, *26*, 525–545. [CrossRef]
10. Feeny, B.; Guran, A.; Hinrichs, N.; Popp, K. Historical review on dry friction and stick–slip phenomena. *Appl. Mech. Rev.* **1998**, *51*, 321–341. [CrossRef]
11. Nakano, K. Two dimensionless parameters controlling the occurrence of stick-slip motion in a 1-DOF system with Coulomb friction. *Tribol. Lett.* **2006**, *24*, 91–98. [CrossRef]
12. Nakano, K.; Maegawa, S. Occurrence limit of stick-slip: Dimensionless analysis for fundamental design of robust-stable systems. *Lubr. Sci.* **2010**, *22*, 1–18. [CrossRef]
13. Kado, N.; Sato, N.; Tadokoro, C.; Skarokek, A.; Nakano, K. Effect of yaw angle misalignment on brake noise and brake time in a pad-on-disc-type apparatus with unidirectional compliance for pad support. *Tribol. Int.* **2014**, *78*, 41–46. [CrossRef]
14. Nakano, K.; Maegawa, S. Stick-slip in sliding systems with tangential contact compliance. *Tribol. Int.* **2009**, *42*, 1771–1780. [CrossRef]
15. Popp, K.; Rudolph, M. Vibration control to avoid stick-slip motion. *J. Vib. Control* **2004**, *10*, 1585–1600. [CrossRef]
16. Kruse, S.; Tiedemann, M.; Zeumer, B.; Reuss, P.; Hetzler, H.; Hoffmann, N. The influence of joints on friction induced vibration in brake squeal. *J. Sound Vib.* **2015**, *340*, 239–252. [CrossRef]
17. Yang, L.; Li, H.; Ahmadian, M.; Ma, B. Analysis of the influence of engine torque excitation on clutch judder. *J. Vib. Control* **2015**, *23*, 645–655. [CrossRef]
18. Maegawa, S.; Itoigawa, F. Design method for suppressing stick-slip using dynamic vibration absorber. *Tribol. Int.* **2019**, *140*, 105866. [CrossRef]
19. Den Hartog, J.P. *Mechanical Vibrations*; McGraw-Hill: New York, NY, USA, 1956.
20. Harik, R.S.; Issa, J.S. Design of a vibration absorber for harmonically forced damped systems. *J. Vib. Control* **2015**, *21*, 1810–1820. [CrossRef]